A High-Range-Accuracy and High-Sensitivity Harmonic Radar Using Pulse Pseudorandom Code for Bee Searching

Zuo-Min Tsai, *Member, IEEE*, Pei-Hung Jau, *Member, IEEE*, Nai-Chung Kuo, *Student Member, IEEE*, Jui-Chi Kao, *Member, IEEE*, Kun-You Lin, *Member, IEEE*, Fan-Ren Chang, *Senior Member, IEEE*, En-Cheng Yang, and Huei Wang, *Fellow, IEEE*

***Abstract*—This paper presents a 9.4/18.8-GHz harmonic radar to investigate the behavior of bees with colony collapse disorder. The challenges of using harmonic radar for bee searching include the requirements of high range accuracy and high sensitivity. A new harmonic radar using the pseudorandom code positioning technique to simultaneously achieve high range accuracy and high sensitivity is proposed. This study also proposes a new method to cancel the local leakage to further improve sensitivity. To realize the transponder, a compact antenna is designed using the topology characteristics of the composite right/left-handed transmission-line concept. The measured sensitivity of the transceiver is −120 dBm, which is 27 dB lower than the noise level. Field testing results demonstrate a 60-m detection range within 1-m distance error with 1.75-W transmitting power. The significant improvement of the sensitivity and the range accuracy reveal the advantages of applying the code-positioning technique to the harmonic radar.**

***Index Terms*—Harmonic radar, pseudorandom code (PRN code), sensitivity, transponder.**

I. Introduction

HARMONIC radars are used to search for the positions of small species [1]–[6]. This study reports the use of harmonic radars to investigate the behavior of bees with colony collapse disorder (CCD), in which worker bees abruptly disappear from a beehive [7]. The operating principle of a harmonic radar is to use a transponder to double the fundamental frequency of the transmitting signal from the transceiver and use it as the receiving signal of the transceiver. The transponders can be detected without the influence of environmental reflection because the unwanted reflection signals from these objects are included in the fundamental frequency and can be filtered. Radar techniques make it possible to determine the distances and the directions of the transponders. Therefore, the positions of targets can be obtained.

Several radar techniques can be used to determine the distance of a harmonic radar transponder. In [3] and [5], the distances were obtained from the power ratio of the transmitting and receiving signals. Although these systems are simple, they are sensitive to the environment or system loss and have low range accuracy. The approaches in [4], [6], and [8] measure the time delays between the envelopes of the transmitted and received pulsed signals. Although time delays are not related to the signal power level, the shortest detection distances are limited by the pulsed widths. In [1], a biased transponder reduced the transmission power of the high accuracy FMCW radar technique. However, this type of a high-power CW source is not easy to obtain.

In summary, accuracy and detection ranges remain challenges for harmonic radars. Accuracy is important because the targets are small. Thus, high accuracy can achieve more accurate positioning. Because the conversion rate of the passive transponder is low, the output power or sensitivity must be increased to improve the detection range.

We propose a new harmonic radar using the pseudorandom code (PRN code) [12], [13] positioning technique, which is one of a spread spectrum technique [16], [17] to achieve high accuracy and high sensitivity simultaneously [9]. Using the correlation of PRN codes, the distances of the bees can be obtained with high range accuracy. Changing the continuous PRN code signal to the pulsed continuous PRN code signal reduces the average power according to the duty cycle of the signal. The processing gain from the correlation of PRN codes improves the sensitivity with the chip number. A new method to cancel the local leakage is also proposed so as not to degrade the sensitivity of the radar. To put the transponder on a bee, a small and lightweight transponder was designed to minimize the effect on

Manuscript received July 10, 2012; revised November 05, 2012; accepted November 05, 2012. Date of publication December 12, 2012; date of current version January 17, 2013. This work was supported in part by National Taiwan University under Excellent Research Projects 98R0062-01 and 98R0062-03 and the National Science Council of Taiwan, R.O.C., under Contract NSC 98-2219-E-002-005, Contract NSC 98-2219-E-002-010, Contract NSC-101-2221-E-194-042, and Contract NSC 98-2221-E-002-059-MY3. This paper is an expanded paper from the IEEE MTT-S International Microwave Symposium, Montreal, QC, Canada, June 17–22, 2012.

Z.-M. Tsai was with the Department of Electrical Engineering and Graduate Institute of Communication Engineering, National Taiwan University, Taipei 106, Taiwan. He is now with the Department of Electrical Engineering and Advanced Institute of Manufacturing with High-tech Innovations, National Chung Cheng University, Chiayi 62102, Taiwan. (e-mail: zuomintsai@gmail.com).

P.-H. Jau and F.-R. Chang are with the Department of Electrical Engineering, National Taiwan University, Taipei 106, Taiwan.

N.-C. Kuo was with Graduate Institute of Communication Engineering, National Taiwan University, Taipei 106, Taiwan. He is now with the University of California, Berkeley, CA USA.

J.-C. Kao, K.-Y. Lin, and H. Wang are with the Graduate Institute of Communication Engineering, National Taiwan University, Taipei 106, Taiwan (e-mail: hueiwang@ntu.edu.tw).

E.-C. Yang is with the Department and Graduate Institute of Entomology, National Taiwan University, Taipei, 106, Taiwan.

Color versions of one or more of the figures in this paper are available online at http://ieeexplore.ieee.org.

Digital Object Identifier 10.1109/TMTT.2012.2230020

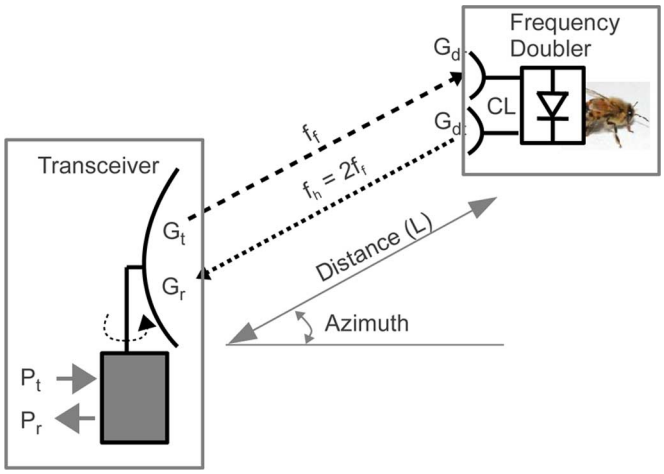

Fig. 1. Configuration of this harmonic radar.

the body of the bee. The proposed 9.4/18.8-GHz harmonic radar achieves transceiver sensitivity of −120 dBm, which is 27 dB lower than the −93-dBm noise level. Field testing shows that the detection range is 60 m with a 1.75-W transmit power. The sensitivity is −106 dBm, which is 13 dB lower than the noise level of −93 dBm. This improvement in sensitivity achieves a 150% improvement in the detection range, which is expected to be 900 m when the output power is 3 kW. Therefore, the PRN code positioning technique significantly improves the accuracy and detection range.

II. System Architecture

Fig. 1 shows the configuration of the proposed harmonic radar. A microwave signal with a power of (P_t) is transmitted to a transponder on a bee, and the transponder doubles the received signal frequency. The distance (L) can be estimated with the received signal from the transponder. The bees can be located using the azimuth determined by the direction of the high-directivity receiving antenna.

The fundamental frequency of the proposed harmonic radar is 9.4 GHz. This selection is a tradeoff between the transponder size, the azimuth resolution, and power budget. The transponder size is an important specification because the transponders must be placed on bees during field tests. To minimize the influence of the bees' movement, the transponders is smaller than 3 mm × 5 mm $(0.09\lambda \times 0.15\lambda)$, which is feasible to design. A high-gain antenna is required to achieve a high-azimuth resolution. Because the directivity of the antenna is inversely proportional to λ^2 and proportional to the effective area, a higher operation frequency can increase the antenna directivity with the same effective area. For a 1.8-m-diameter dish antenna operating at 9.4 GHz, the antenna directivity is greater than 38 dB and the 3-dB beamwidth is smaller than 1°. Because the periphery of 1° with a radius of 100 m is 1.7 m, this azimuth resolution satisfies the purpose of this harmonic radar to search for bee searching. However, increasing the operation frequency decreases the received power according to the Friis formula and increases the difficulty of achieving a high-power amplifier. Therefore, the 9.4-GHz operating frequency is selected for this bee-searching radar to achieve a reasonable searching distance and azimuth resolution.

According to the Friis formula, the received power (P_r) can be expressed as

$$P_r = \frac{P_t G_t}{4\pi L^2} A_{df} E_{dh} G_{dh} \frac{A_r}{4\pi L^2} \tag{1}$$

where G_t is the antenna gain of the transmitting antenna, A_r is the effective area of the receiving antenna, A_{df} is the effective area of the transponder in fundamental frequency, G_{dh} is the antenna gain of the transponder at the second-harmonic frequency, and E_{dh} is the conversion efficiency of the diode. Expressing the effective area of antenna to the gain of antenna and the wavelength, the Friis formula can be written as

$$P_r = P_t G_t G_r \left(\frac{\lambda_f}{4\pi L}\right)^2 G_{df} E_{dh} G_{dh} \left(\frac{\lambda_h}{4\pi L}\right)^2. \tag{2}$$

The conversion rate of the transponder is defined as the ratio between the total radiated power from the transponder to the power density of the transponder. If the sensitivity of the transceiver is P_{rmin}, then the detection range $R_{\max}$ can be expressed as

$$R_{\max} = \frac{1}{4\pi}\left(\frac{P_t G_t G_r G_{df} E_{dh} G_{dh} \lambda_f^2 \lambda_h^2}{P_{\mathrm{rmin}}}\right)^{\frac{1}{4}}. \tag{3}$$

Since E_{dh} degrades with the power density rapidly, a high P_t is required to extend the detection range. However, the cost of the power amplifier with high P_t is high. Thus, this study proposes using a PRN code radar to improve P_{rmin} so that $R_{\max}$ can also be improved without increasing P_t.

III. Pulsed PRN Code Radar Principle

PRN code is a radar technique of pulse compression to accurately estimate the delay (τ) between the transmit and receive signal. Comparing the other code techniques, such as Barker code [14] and Gold code [15], the PRN code technique has the advantage of being easily generated and high accuracy. The distance (L) between the target and the transceiver can be calculated as

$$L = (c \times \tau)/2 \tag{4}$$

where c is the speed of the microwave signal. The reason of using the PRN code is that the correlation function of PRN code provides significantly better sensitivity and distance accuracy [18].

Fig. 2(a) shows the waveform of the PRN code (C_x) used in the proposed radar. This PRN code is a pseudo-random sequence with 1023 chips. The chipping rate (f_{code}) is 25 MHz, and, as a result, the total length of PRN code is approximately

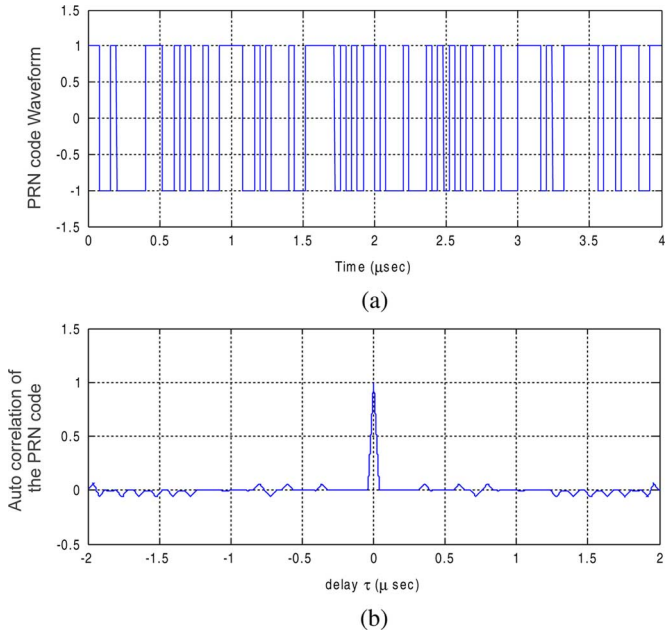

Fig. 2. (a) Waveform and (b) autocorrelation of the PRN code.

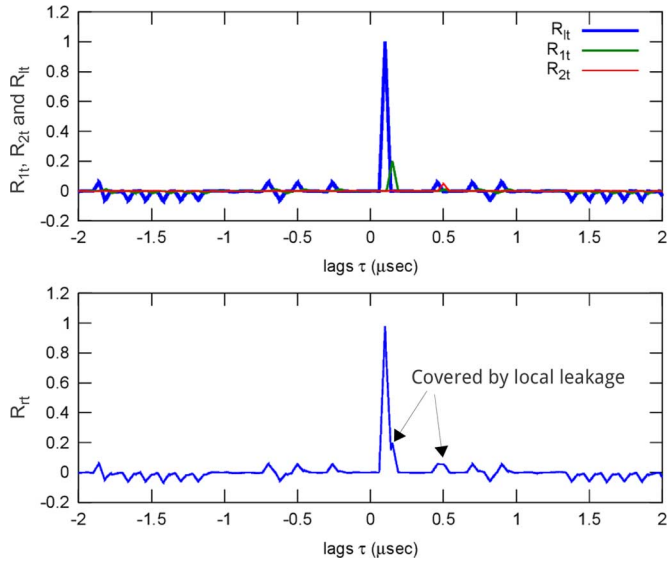

Fig. 3. Correlation of the received signal including multiple targets and the influence of the correlation cause by the local leakage.

40 μs. Fig. 2(b) shows the autocorrelation (R_{xx}) of C_x defined as

$$R_{xx}(t) = \int C_x(t)C_x(t-\tau). \tag{5}$$

R_{xx} is close to 1 when τ is zero and decreases rapidly when τ is away from zero. When τ is away from zero to one chip width $T_{\text{code}}(1/f_{\text{code}})$, the absolute value of the autocorrelation function decreases by less than $65/1023 = 0.064$ [10]. This property is important to calculate the delay between two identical PRN code signals with time delay. For example, by calculating the correlation between the transmitted signal (C_t) and the received signal (C_r), the delay between C_t and C_r can be found by searching the peak of the correlation. Because the correlation between C_r and C_t decreases rapidly while τ is away from the delay between C_r and C_t, the time resolution is determined by the sampling rate of the waveform. A 8-b oscilloscope with a sampling rate of 2 GHz is used to capture the waveforms. Consequently, the time resolution of the delay is 0.5 ns. This time resolution leads to a high ideal range accuracy of 7.5 cm, according to (4).

In addition to the advantage of high range accuracy, applying the PRN code can also improve the sensitivity of the radar. When calculating the autocorrelation of the PRN code, the processing gain is proportional to the number of chips [10]. On the other hand, the system has a 30-dB processing gain upon applying the PRN code with 1023 chips. This 30-dB processing gain enables the radar system to detect the received signals with the power level of 30 dB below the noise level theoretically. This significantly expends the detection range without increasing the output power.

To apply the PRN code to this radar system, the PRN code is modified from a continuous signal to a pulsed signal with a duty cycle of 5%. Therefore, the average output power is 1/20 of the peak output power. The reason of this modification is that a high-power pulsed microwave amplifier is more readily available than a high-power CW microwave amplifier. The 5% duty cycle pulsed signal has a repeating period of 1 ms.

When C_r includes signals from multiple targets, such as

$$C_r = \sum_{i=1}^{n} C_{ri} \tag{6}$$

the correlation between C_r and C_t is the sum of the correlation between each reflection signal and C_r as follows:

$$R_{rt} = \sum_{i=1}^{n} R_{it}. \tag{7}$$

This is because the correlation in (5) is a linear transformation. As shown in Fig. 3, the correlation between C_r and C_t exhibits multiple peaks when there are multiple targets. The peak values of the correlation are proportional to the magnitude of the signal from the targets. The number and delays of the multiple target signals can be found by observing the number of the peaks and the delays of the peaks.

The linearity of this correlation can be used to detect the multiple targets and cancel unwanted signals from the local leakage. Fig. 3 illustrates the correlation between C_t and C_r, which contains signals from local leakage and targets. The power level of the local leakage is usually much higher than the target signal power. Thus, if the delay between the target signal and the local leakage is too short, the correlation related to the target signal (R_{1t}) will be covered by the correlation related to the local leakage (R_{lt}). Because the correlation is not equal to zero (maximum to 1/100) [Fig. 2(b)] when the delay is far from zero, the correlation related to the far target signal (R_{2t}) will still be covered by (R_{lt}). Because both the peak of the near target correlation and the peak of the far target correlation are influenced by the local leakage correlation (R_{lt}), the cancellation of the

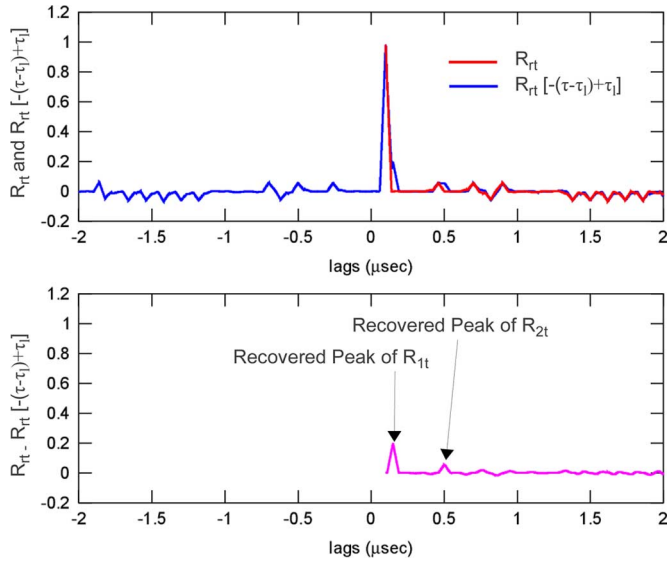

Fig. 4. Proposed local leakage cancellation using the symmetric property of the local leakage autocorrelation.

local leakage is necessary to prevent the local leakage from influencing the sensitivity of the radar.

This study proposes a new method of canceling the local leakage. Because the linearity of the correlation, the correlation related to the local leakage can be subtracted from R_{rt}. According to Fig. 2(b), the autocorrelation of the PRN code is symmetric with respect to τ of zero. Therefore, the correlation related to the local leakage (R_{lt}) with delay of τ_l is symmetric with respect to τ of τ_l and can be expressed as

$$R_{lt}(\tau) = R_{lt}[-(\tau - \tau_l) + \tau_l]. \tag{8}$$

Consider a correlation (R_{rt}) containing the summation related to R_{lt} and multiple target $(R_{it}(\tau))$ expressed as

$$R_{rt}(\tau) = R_{lt}(\tau) + \sum_{i=1}^{n} R_{it}(\tau). \tag{9}$$

By subtracting the correlation mirror to R_{rt} at τ_l, R_{lt} in R_{rt} can be canceled effectively. The derivation is expressed as

$$\begin{aligned} &R_{rt}(\tau - \tau_l) - R_{rt}[-(\tau - \tau_l) + \tau_l] \\ &\quad = \{R_{lt}(\tau) - R_{lt}[-(\tau - \tau_l) + \tau_l]\} \\ &\qquad + \sum_{i=1}^{n} \{R_{it}(\tau) - R_{it}[-(\tau - \tau_l) + \tau_l]\} \\ &\quad \approx \sum_{i=1}^{n} R_{it}(\tau). \end{aligned} \tag{10}$$

and the process is illustrated in Fig. 4.

IV. Harmonic Radar Implementation

Fig. 5 shows a block diagram of the proposed harmonic radar system. A pulsed PRN code (C_t) is generated with an FPGA board. The rise time is 10 ns and the fall time is 14 ns. This PRN code modulates a 9.4-GHz CW wave that in turn produces a pulsed RF signal. A traveling-wave-tube (TWT) high-power amplifier with peak output power of 3 kW was applied to amplify the output signal from the transmitter to increase the searching range. This TWT high-power amplifier is a pulsed power amplifier with a maximum pulse width of 50 μs and a maximum duty cycle of 5%. After being amplified to a high power level with the high-power amplifier, the pulse RF signal passes through a low pass filter to remove the unwanted second harmonic. The transponders receive the pulse RF signal and double the frequency to 18.8 GHz. The 18.8-GHz signal from the transponder is received by the receiver and demodulated to a received PRN code (C_r^I, and C_r^Q). A four-channel, 2-GHz sampling rate scope receives the trigger signals C_t, C_r^I and C_r^Q and transfers the received signal to a computer to calculate the distance.

The modulation selected in this harmonic radar is binary phase-shift keying (BPSK) modulation. The transponders double both the frequency and the phase of the RF signal. Therefore, the modulator in the transmitter must be modified from a BPSK modulator to 0° and 90° phase-shift keying modulator to convert the output signals from transponders to BPSK signals.

An IQ mixer and not a balanced mixer is required to demodulate the BPSK-modulated signal from the transponders. If a balanced mixer is used for demodulation, the output signal will be null at some distance which creates 90° or 270° phase difference between the received signal and the LO of the demodulator. With the IQ mixer, the distance of null output signal in I channel C_r^I and Q channel C_r^Q are complementary. Therefore, the results of both C_r^I and C_r^Q can cover the measured distance without null output signal. Table I lists the requirements of the components in the harmonic radar. Frequency multipliers in the LO chains are used separately for the modulator and the demodulator to reduce the local leakage from the LO chain. Therefore, most of the 9.4-GHz leakage RF signal of the modulator is suppressed in the input of the frequency multiplier. Fig. 6 shows a photograph of the transceiver integrated in a metal box.

In the field test, the transceiver is connected to a high-gain antenna with a diplexer. Therefore, the local leakage from the diplexer has to be further suppressed because the power level of the high-power amplifier is very high so that the second harmonic is higher than the reflection signal from the transponders. In addition to the diplexer, two 50-dB suppression low-pass filters are used to connect with a wideband isolator to achieve more than 100-dB total second-harmonic suppression. Although local leakage from the diplexer is reduced, it still cannot be neglected. Therefore, the cancellation method for the local leakage described in Section II is applied to cancel the local leakage.

Regarding the application of the transponders, the load bearing of bees limit the transponder size to 3 mm × 5 mm. To improve the conversion rate in low power density, a silicon Schottky diode with barrier voltage lower than 0.2 V is used for the frequency doubler. Because the transponders are mounted on bees, it is necessary to reduce the influence of the radiation

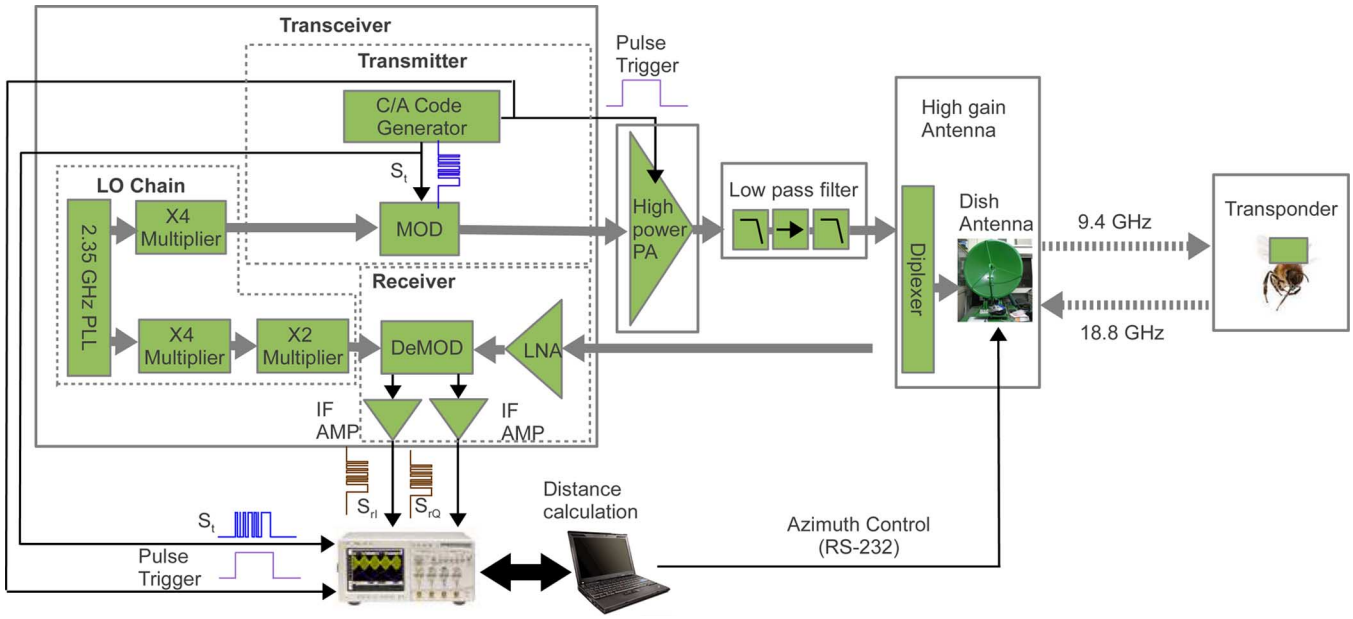

Fig. 5. Block diagram of this radar system.

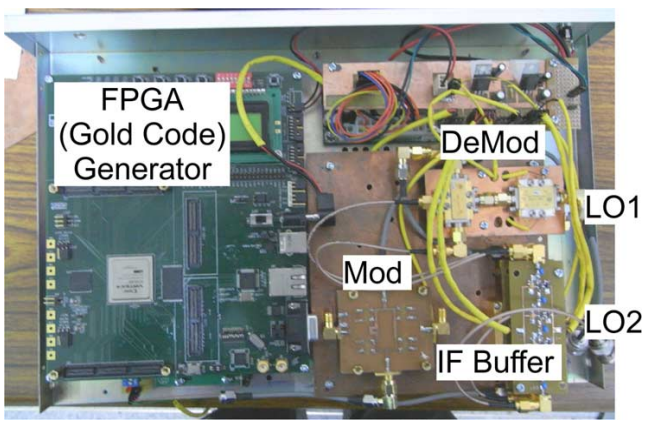

Fig. 6. Photograph of the transceiver.

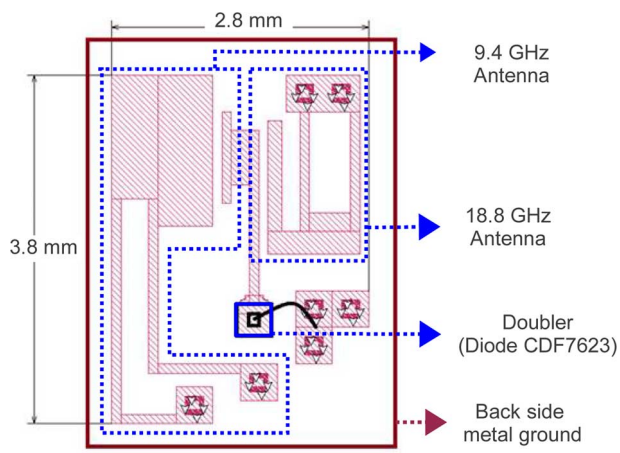

Fig. 7. Layout of the transponder.

TABLE I
SPECIFICATION OF THE COMPONENTS IN THE HARMONIC RADAR

High Power Amplifier	Gain 75 dB	Output Power 65 dBm
Modulator	Conversion Gain -9 dB	Output Power -6 dBm
Antenna	Antenna Gain (9.4 GHz) 38 dB	Antenna Gain (18.8 GHz) 43 dB
Diplexer	Insertion Loss 0.5 dB	Isolation 60 dB
LNA	Gain 40 dB	Noise Figure 3 dB
IQ Mixer	Conversion Gain -8 dB	
IF amplifier	Gain 60 dB	Bandwidth 100 MHz

pattern caused by bees' bodies. Thus, the antenna is designed by using the composite right-/left-handed transmission-line (CRLH TL) concept [11], which has a complete backside ground metal to shield the bees' bodies. Fig. 7 shows the layout of the transponder. This transponder is designed on a 30-mil Ro3003 substrate. Both 9.4- and 18.8-GHz antennas are realized in an area of 2.8 mm $\times$ 3.8 mm with 20-mg weight. This weight could be reduced by using other low-weight material as the substrate of the antenna. This 20-mg weight is about 20% of the weight of a bee and has to be carefully taken into consideration while designing the related entomology experiments [19] and [20]. Fig. 8 shows the simulated radiation pattern. A box of water was placed under the transponder to simulate of the antenna gain accounted for the body of the bee. The simulated pattern is omnidirectional in the XY plane, with the antenna gain of -5 dBi. To measure the transponder, a transponder is placed at a distance to a standard gain horn antenna. A CW signal in 9.4 GHz is transmitted to the standard gain horn antenna. To separate the transmitting and the receiving power, a directional coupler is used in front of the standard gain horn antenna. A spectrum analyzer is applied on the coupled port of

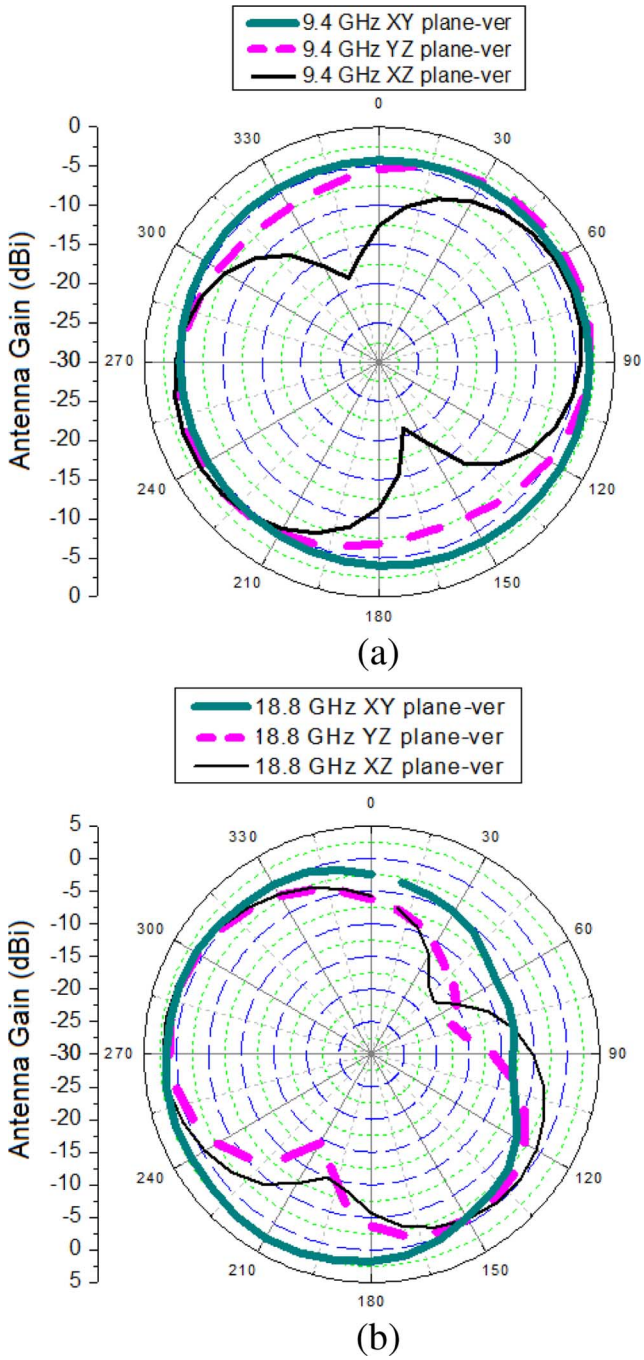

Fig. 8. Simulated pattern of the dual band antenna.

the coupler to measure the power level of the receiving power. Using (2) and the measured receiving power level, $G_{df}E_{dh}G_{dh}$ is estimated to be -34 dB at a power density of 1 W/mm^2. Using the simulated antenna gain of -5 dBi, the doubler conversion rate E_{dh} is estimated to -24 dB and the degradation of the conversion gain due to the bee body is only 3 dB.

Fig. 9 shows the photographs of transponders and one transponder on a bee. The size of the transponder is compact enough that 16 transponders can be placed on a coin of 20-mm diameter. To avoid influencing the wing movement of the bee, the transponder is mounted on the back of the abdomen. Several field tests show that bees are able to fly as well as go in and out of the beehive wearing the transponders.

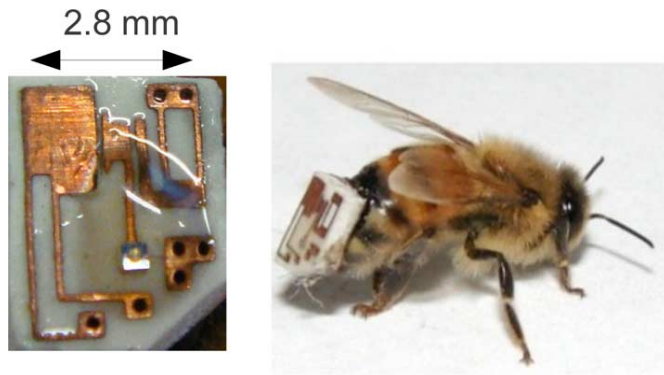

Fig. 9. Photograph of the transponder.

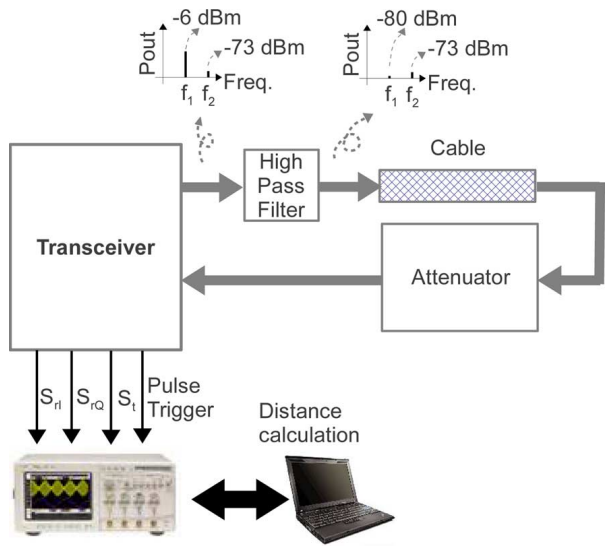

Fig. 10. Measurement setup for the sensitivity of the transceiver.

V. Measurement

A. Transceiver Sensitivity

Before the field test, we measured the sensitivity of the transceiver in the laboratory. The major difficulty in measuring the sensitivity is that the frequency of the transmitting signal must be doubled to be the receiving signal. However, the conversion rate (E_{dh}) of the frequency doubler is sensitive to the input power, especially when the input power is low. Therefore, we reused the second harmonic of the transmitting signal as the receiving signal directly. Fig. 10 shows the measurement setup for the sensitivity. The transmitting signal is connected to a high pass filter to remove the signal in fundamental frequency. The power level of the fundamental signal is then suppressed to -80 dBm, which is 7 dB below the -73-dBm power level of the second-harmonic signal. Because the signal after the filter is dominated by the second-harmonic signal, it can be used as the receiving signal. After the filter, a cable of 2-m length is used to emulate the time delay between the transmitting and the receiving signal. To control the input power of the receiving signal, different attenuators are used after the cable.

Fig. 11 illustrates the measured waveforms of the received I and Q signals. The difference between the signal and the noise

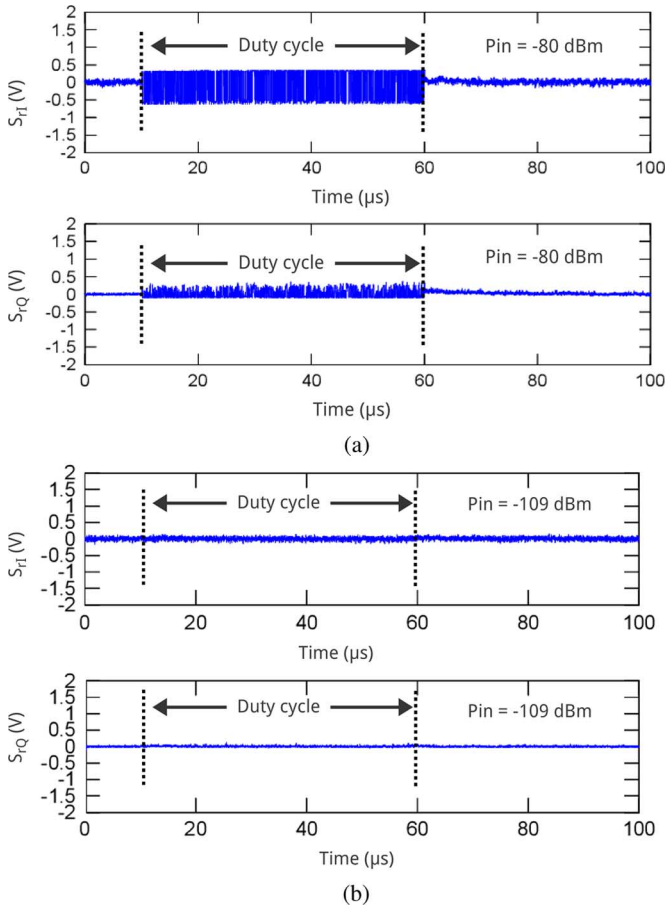

Fig. 11. Measured waveform with (a) −80- and (b) −109-dBm input power.

is apparent in the difference of the waveform inside and outside the duty cycle. Because the bandwidth of the IF amplifier is 100 MHz, the noise level is approximately −93 dBm. Therefore, the signal is much higher than the noise when the input power is −80 dBm. On the other hand, there is no difference in the waveform with and without the duty cycle when the input power is −109 dBm because the signal power is below the noise level.

Fig. 12 shows the standard deviation of the delay and the mean of the peak value relating to the peak correlation versus receiving power over twenty measurements. Because the IF amplifier is designed to limit the output voltage to ±1.4 V, the peak value is limited to the same level when the input power exceeds −90 dBm. Conversely, the peak value is proportional to the square of the input power when the input power is lower than −90 dBm because the correlation is proportional to the receiving voltage. The minimum measured peak value is 0.03 with a −124-dBm input power. The standard deviation is still smaller than two sample numbers when input power is higher than −120 dBm. This −120 dBm input power is 27 dB higher than the −93-dBm noise level and verifies the 30-dB processing gain while calculating the correlation of the PRN codes.

B. Field Test

Fig. 13(a) shows an aerial map of the area for the field test. Because the longest distance of this area is 70 m, couplers and

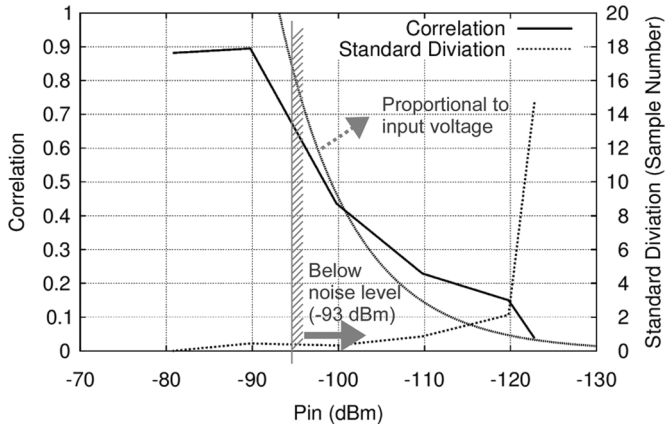

Fig. 12. Standard deviation of the delay and the mean of the peak value relating to the peak correlation versus receiving power in 20 measurements.

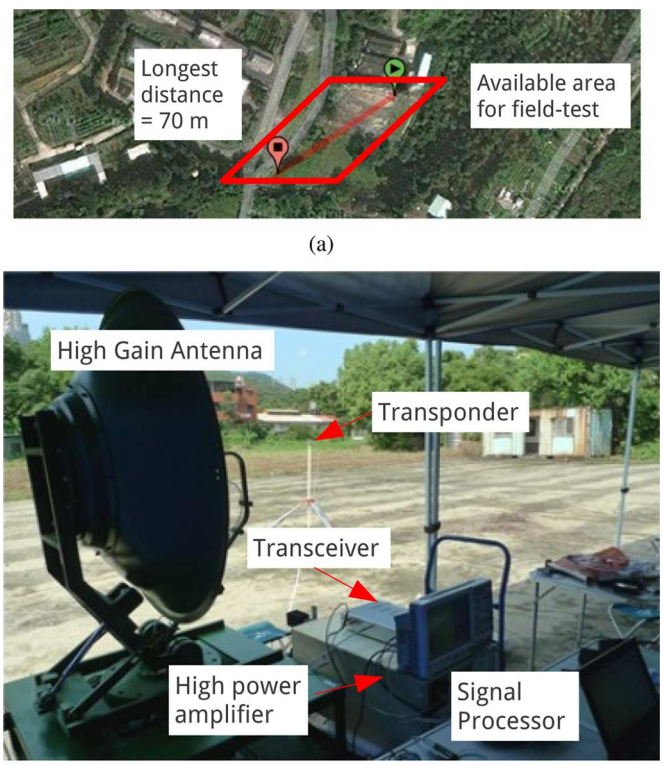

Fig. 13. (a) Aerial map and (b) setup of the field test.

attenuators are applied to the 3-kW power amplifier to decrease the output power to 1.75 W. We used this harmonic radar to find the fixed position of the transponder fixed away from the transceiver as shown in Fig. 13(b).

Although a high-rejection low-pass filter was applied to the output of the high-power amplifier (Fig. 5), the power level of the leaking second-harmonic signal from the high-power amplifier through the diplexer is still high compared with the signal received from the transponder. Therefore, the leakage cancellation described in Section II is important to prevent the leakage from influencing the measurement results. Fig. 14 shows the function of the leakage cancellation when measuring the transponder 50 m away from the transceiver. The dominate

TABLE II
COMPARISON TABLE OF THE PUBLISHED HARMONIC RADAR

Ref.	Freq. (GHz)	Positioning Technique	Peak Power (W)	Duty Cycle	Detection Range (m)	Ideally Range Accuracy (m)	Transponder Size (mm × mm)
[1]	5.3 / 10.6	FMCW	1	100%	*1080	N.A.	*30 × 30
[3]	5.9 / 11.9	Received Power	0.1	100%	60	N.A.	9.5 × 9.5
[5]	0.91 / 1.82	Received Power	1	100%	2	N.A.	(wire) 80
[8]	9.4 / 18.8	Pulse Radar	25 k	0.015%	900	3.75	(wire) 16
This work	9.4 / 18.8	Pulse PRN code	1.75	5%	60	0.075	2.8 × 3.8
This work (expected)	9.4 / 18.8	Pulse PRN code	3 k	5%	900	0.075	2.8 × 3.8

* Using biased transponders.

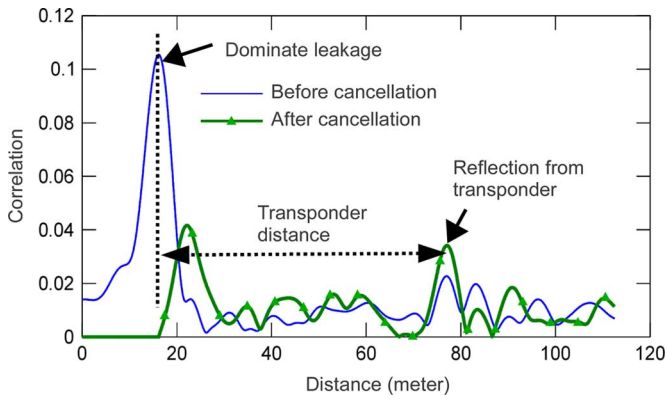

Fig. 14. Verification of the leakage cancellation function.

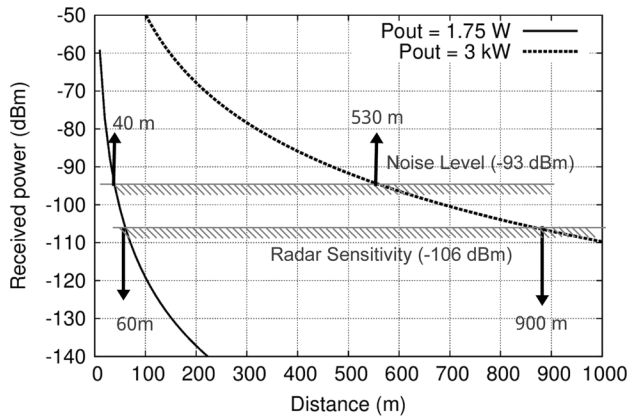

Fig. 16. Receiving power versus distance.

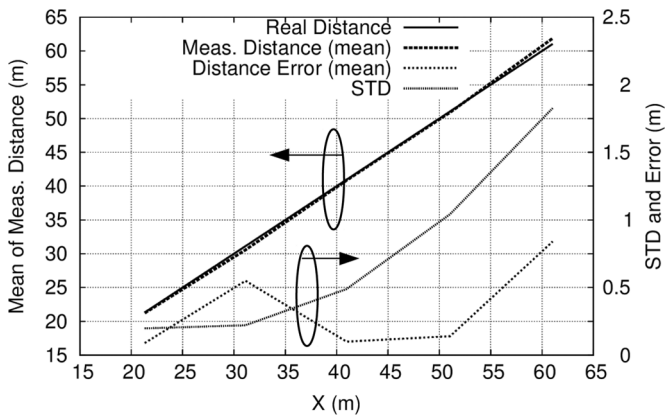

Fig. 15. Comparison between the real and measured distance.

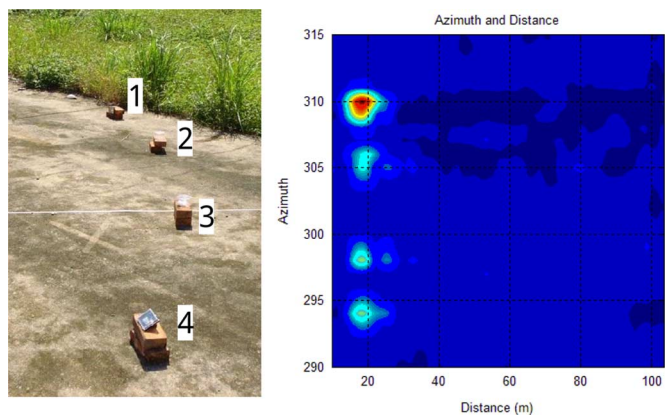

Fig. 17. Measurement results with multiple transponders.

leakage was first found and then cancelled according to the property of the symmetry. After the leakage cancellation, the peak of the leakage signal in short distance is cancelled. The difference between the peak value from the transponder at 75 m distance and unwanted peak value near the transponder is also reduced. Because the correlation of the local leakage is negative at the distance of 75 m, the peak value from the transponder at 75 m is increased after leakage cancellation. Therefore, the leakage cancellation confirms that the dominate leakage will not influence the measurement results. According to the half pulse width of Fig. 14, the resolution of this radar system is estimated to be 6 m.

Fig. 15 shows a comparison of the real and measured distances from the radar. The measured distance is the mean of 20 measurements and is close to the real distance. Within a distance of 61 m, the errors are below 1 m and the standard deviation is less than 2 m which are acceptable for bee-searching application.

In Fig. 16, the receiving power versus distance with transmitting power for both 1.65 W and the 3 kW is calculated according

to (2). The receiving power at the 61-m maximum detection range in the field test is estimated to be −106 dBm, which is 13 dB higher than the −93-dBm noise level. The 13-dB improvement of the sensitivity improves the distance from 40 to 61 m. The reason to use this estimation is that the weak received power is below the noise level and cannot be directly measured with the spectrum analyzer. This estimation can be verified by comparing the results from the transceiver sensitivity measurement (Fig. 12). The estimated sensitivity of the radar (−106 dBm) is worse than the measured transceiver sensitivity (−120 dBm). This is reasonable because the transponder position for the best receive power is difficult to be achieved in the field test. Using the estimated sensitivity of the radar and the received power versus distance with 3 kW transmitting power, the detection distance can then be estimated. If the 3-kW output power is applied, the detectable range increases from 530 to 900 m because the sensitivity is 13 dB higher than the −93-dBm noise level. This improvement alleviates the high power requirements of the harmonic.

Finally, the measurement results with multiple transponders were performed with four transponders putting in different positions (Fig. 17), which reveal that all of the transponders are found during the measurement.

Table II presents a comparison of the published harmonic radar, showing that the proposed PRN code harmonic radar achieves high range accuracy and small transponder size.

VI. Conclusion

This study presents a 9.4/18.8-GHz harmonic radar for bee searching. This harmonic radar uses the PRN code position technique to achieve high range accuracy and high sensitivity simultaneously. The ideal range accuracy for this harmonic radar is 0.075 m, which is determined by the sampling rate of the IF signal. Calculating the correlation between the PRN codes shows that a 30-dB processing gain is achieved, and the sensitivity is improved to −120 dBm. A transponder using the CRLH TL concept is designed to reduce the antenna size and minimize the influence of radiation pattern from the bee body. Field tests achieved a 61-m detection range is achieved at a 1.75-W transmission power with only 1-m distance error and 2-m standard deviation. Therefore, it is confirmed that the proposed PRN code positioning technique improves the range accuracy and the detection range.

References

[1] N. Tahir and D. G. Brooker, "Recent developments and recommendations for improving harmonic radar tracking systems," in *Proc. 5th Eur. Conf. Antennas Propag.*, Apr. 2011, pp. 1531–1535.

[2] A. Lai, K. M. K. H. Leong, and T. Itoh, "Harmonic radar transceiver design: Miniature tags for insect tracking," *IEEE Trans. Antennas Propag.*, vol. 52, no. 11, pp. 2825–2832, Nov. 2004.

[3] D. Psychoudakis, W. Moulder, C.-C. Chen, H. Zhu, and J. L. Volakis, "A portable low-power harmonic radar system and conformal tag for insect tracking," *IEEE Trans. Antennas Propag.*, vol. 52, no. 11, pp. 2825–2832, Nov. 2004.

[4] J. R. Riley, D. R. Reynolds, A. S. Edwards, J. L. Osborne, I. H. Williams, N. L. Carreck, and G. M. Poppy, "Tracking bees with harmonic radar," *Nature*, vol. 379, pp. 29–30, Jan. 1996.

[5] J. Kiriazi, J. Nakakura, K. Hall, N. Hafner, and V. Lubecke, "Low profile harmonic radar transponder for tracking small endangered species," in *Proc. IEEE Eng. Medicine Biol. Soc. 29th Annu. Int. Conf.*, Aug. 2007, no. 22–26, pp. 2338–2341.

[6] O. Ovaskainena, A. D. Smith, J. L. Osborneb, D. R. Reynoldsc, N. L. Carreckb, A. P. Martinb, K. Niitepolda, and I. Hanskia, "Tracking butterfly movements with harmonic radar reveals an effect of population age on movement distance," in *Proc. Nat. Acad. Sci. Symp.*, Dec. 2008, vol. 105, no. 49, pp. 19090–19095.

[7] J. L. Osborne, S. J. Clark, R. J. Morris, I. H. Williams, J. R. Riley, A. D. Smith, D. R. Reynolds, and A. S. Edwards, "A landscape-scale study of bumble bee foraging range and constancy, using harmonic radar," *J. Appl. Ecol.*, vol. 36, no. 4, pp. 519–533, Sept. 1999.

[8] J. R. Riley and A. D. Smith, "Design considerations for an harmonic radar to investigate the flight of insects at low altitude," *Comput. Electron. Agriculture*, vol. 35, pp. 151–169, 2002.

[9] Z.-M. Tsai, P.-H. Jau, N.-C. Kuo, J.-C. Kao, K.-Y. Lin, F.-R. Chang, E.-C. Yang, and H. Wang, "A high range resolution 9.4/18.8 GHz harmonic radar for bees searching," in *IEEE MTT-S Int. Microw. Symp. Dig.*, Montreal, QC, Canada, Jun. 2012, pp. 1–3.

[10] P. Misra and P. Enge, *Global Positioning System: Signals, Measurements, and Performance*. Lincoln, MA: Ganga-Jamuna, 2006, pp. 356–359.

[11] A. Lai, K. M. K. H. Leong, and T. Itoh, "Infinite wavelength resonant antennas with monopolar radiation pattern based on periodic structures," *IEEE Trans. Antennas Propag.*, vol. 55, no. 3, pp. 868–876, Mar. 2007.

[12] H.-J. Zepernick and A. Finger, *Pseudo Random Signal Processing: Theory and Application*. New York: Wiley, 2005.

[13] M. J. Dorsett, "Radar processing of $2^n - 1$ and 2^n PRN coded waveforms," in *Proc. 13th Int. Conf. Microw., Radar and Wireless Commun.*, 2000, vol. 2, pp. 623–626.

[14] M. W. Jelffs, "Finite-length binary phase codes for digital pulse compression," *Electron. Lett.*, vol. 12, pp. 197–199, 2011.

[15] T. B. Hale, M. A. Temple, and B. L. Crossley, "Ambiguity analysis for pulse compression radar using gold code sequences," in *Proc. IEEE Radar Conf.*, 2011, pp. 111–116.

[16] J. K. Holmes, *Spread Spectrum Systems for GNSS and Wireless Communications*. : Artech House.

[17] R. L. Peterson, R. E. Ziemer, and D. E. Borth, *Introduction to Spread Spectrum Communications*. Upper Saddle River, NJ: Prentice-Hall, 1995.

[18] D. V. Sarwate and M. B. Pursley, "Cross-correlation properties of pseudorandom and related sequences," *Proc. IEEE*, vol. 68, no. 5, pp. 593–619, May 1980.

[19] G. Boiteau, C. Vincent, F. Meloche, and T. C. Leskey, "Harmonic radar: Assessing the impact of tag weight on walking activity of Colorado potato beetle, plum curculio, and western corn rootworm," *Ecol. Behavior*, vol. 103, no. 1, 2010.

[20] G. Boiteau, C. Vincent, F. Meloche, T. C. Leskey, and B. G. Colpitts, "Evaluation of tag entanglement as a factor in harmonic radar studies of insect dispersal," *Environ. Entomol.*, vol. 40, no. 1, pp. 94–102, 2011.

Zuo-Min Tsai (S'03–M'07) was born in Maioli, Taiwan, in 1979. He received the B.S. degree and Ph.D. degree in communication engineering from National Taiwan University, Taipei, Taiwan, in 2001 and 2006, respectively.

From 2006 to 2011, he was a Postdoctoral Research Fellow with the Graduate Institute of Communication Engineering, National Taiwan University, Taipei, Taiwan. In July 2011, he joined the faculty of the Department of Electrical Engineering, National Chung Cheng University, Chiayi, Taiwan, where he is currently an Assistant Professor. His research interests include the design of microwave integrated circuits and microwave systems.

Pei-Hung Jau (M'12) was born in Tainan, Taiwan, in 1982. He received the B.S. and M.S. degrees in electrical engineering from National Sun Yat-sen University, Kaohsiung, Taiwan, in 2005 and 2007, respectively. He is currently working toward the Ph.D. degree at National Taiwan University, Taipei, Taiwan.

His current research interest is wireless positioning systems.

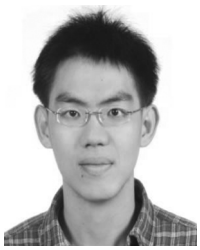

Nai-Chung Kuo (S'09) was born in Taipei, Taiwan, in 1987. He received the B.S. degree in electrical engineering and M.S. degree in communication engineering from National Taiwan University, Taipei, Taiwan, in 2009 and 2011, respectively. He is currently working toward the Ph.D. degree at the University of California, Berkeley.

He served the substitute service in Bureau of Standards, Metrology and Inspection (BSMI), MOEA from 2011 to 2012. His research interests are the design and theory of microwave/millimeter-wave circuits.

Jui-Chi Kao (M'12) was born in Taipei, Taiwan, in 1985. He received the B.S. degree in communication engineering from National Central University, Taoyuan, Taiwan, in 2008. He is currently working toward the Ph.D. degree at National Taiwan University, Taipei, Taiwan.

His research interests include monolithic microwave/millimeter-wave circuit design.

Kun-You Lin (M'12) was born in Taipei, Taiwan, in 1975. He received the B.S. degree in communication engineering from National Chiao Tung University, Hsinchu, Taiwan, in 1998, and the Ph.D. degree in communication engineering from National Taiwan University, Taipei, Taiwan, in 2003.

From August 2003 to March 2005, he was a Postdoctoral Research Fellow with the Graduate Institute of Communication Engineering, National Taiwan University, Taipei, Taiwan. From May 2005 to July 2006, he was an Advanced Engineer with the Sunplus Technology Company Ltd., Hsinchu, Taiwan. Since July 2006, he has been with the faculty of the Department of Electrical Engineering, Graduate Institute of Communication Engineering, National Taiwan University, where he is currently an Associate Professor. His research interests include the design and analysis of microwave/RF circuits.

Dr. Lin is a member of Phi Tau Phi.

Fan-Ren Chang (M'06–SM'12) was born in Taiwan in 1949. He received the B.S. and M.S. degrees from National Chiao Tung University, Hsinchu, Taiwan, in 1972 and 1974, respectively, and the Ph.D. degree from the University of Houston, Houston, TX, in 1985, all in electrical engineering.

He joined the Department of Electrical Engineering, National Taiwan University in 1985 as an associate professor. From 1990, he became a professor at the same department until now. He was the visiting professor of EE Department of Stanford University from October 2002 to February 2003. He is currently a Professor with the Department of Electrical Engineering, National Taiwan University, Taipei, Taiwan. His research interests include linear multivariable systems, generalized systems, numerical algorithms, and satellite navigation systems.

En-Cheng Yang was born in Chia-Yi city, Taiwan, in 1965. He received the B.S. degree in entomology from the National Chung Hsing University, Taichung, Taiwan, in 1988, and the Ph.D. degree in neuroscience from the Australian National University, Canberra, Australia, in 1994.

From September 1994 to June 1996, he was a Postdoctoral Research Fellow with the Centre for Visual Science, Australian National University. He was then a Postdoctoral Research Fellow with Academica Sinica, Taipei, Taiwan, from July 1996 to July 1999. Then, he became a Faculty Member with the Department of Entomology, National Chung Hsing University, as an Assistant Professor, and later became an Associate Professor. In August 2006, he joined the faculty of the Department of Entomology, National Taiwan University, Taipei. In August 2010, he became a Full Professor. His research interests are mainly in neuroethology, especially focusing on the sensation and perception of insect sensory systems and the biology of honey bee. He is also involved some projects working on the applications of wireless sensor networks for insect pest control.

Huei Wang (S83–M87–SM95–F06) was born in Tainan, Taiwan, in 1958. He received the B.S. degree in electrical engineering from National Taiwan University, Taipei, Taiwan, in 1980, and the M.S. and Ph.D. degrees in electrical engineering from Michigan State University, East Lansing, in 1984 and 1987, respectively.

During his graduate studies, he was engaged in research on theoretical and numerical analysis of electromagnetic radiation and scattering problems. He was also involved in the development of microwave remote detecting/sensing systems. He joined the Electronic Systems and Technology Division of TRW Inc. in 1987. He has been an MTS and Staff Engineer responsible for monolithic microwave integrated circuit (MMIC) modeling of compute-aided design tools, and MMIC testing evaluation and design and became the Senior Section Manager of MMW Sensor Product Section of the RF Product Center. He visited the Institute of Electronics, National Chiao-Tung University, Hsin-Chu, Taiwan, in 1993 to teach MMIC-related topics and returned to TRW in 1994. He joined the faculty of the Department of Electrical Engineering, National Taiwan University, Taipei, Taiwan, as a Professor in February 1998. He served as the Director of Graduate Institute of Communication Engineering of National Taiwan University from August 2006 to July 2009.

Dr. Wang is a member of Phi Kappa Phi and Tau Beta Pi. He received the Distinguished Research Award of National Science Council, Taiwan, at 2003. He was the Richard M. Hong Endowed Chair Professor of National Taiwan University in 2005–2007. He was elected as an IEEE Fellow in 2006, and has been appointed as an IEEE Distinguished Microwave Lecturer for the term of 2007–2009. Dr. Wang received the Academic Achievement Award from Ministry of Education, Taiwan, in 2007, and the Distinguished Research Award from Pan Wen-Yuans Foundation in 2008. He is currently a National Chair Professor of Ministry of Education, Taiwan, for the term from February 2011 to January 2014.